Early breakthrough of colloids and bacteriophage MS2 in a water-saturated sand column

Arturo A. Keller and Sanya Sirivithayapakorn

Bren School of Environmental Science and Management, University of California, Santa Barbara, California, USA

Constantinos V. Chrysikopoulos

Department of Civil and Environmental Engineering, University of California, Irvine, California, USA

Received 11 September 2003; revised 20 May 2004; accepted 7 June 2004; published 14 August 2004.

[1] We conducted column-scale experiments to observe the effect of transport velocity and colloid size on early breakthrough of free moving colloids, to relate previous observations at the pore scale to a larger scale. The colloids used in these experiments were bacteriophage MS2 (0.025 μm), and 0.05- and 3-μm spherical polystyrene beads, and were compared with a conservative nonsorbing tracer (KCl). The results show that early breakthrough of colloids increases with colloid size and water velocity, compared with the tracer. These results are in line with our previous observations at the pore scale that indicated that larger colloids are restricted by the size exclusion effect from sampling all paths, and therefore they tend to disperse less and move in the faster streamlines, if they are not filtered out. The measured macroscopic dispersion coefficient decreases with colloid size due to the preferential flow paths, as observed at the pore scale. Dispersivity, typically considered only a property of the medium, is in this case also a function of colloid size, in particular at low Peclet numbers due to the size exclusion effect. Other parameters for colloid transport, such as collector efficiency and colloid filtration rates, were also estimated from the experimental breakthrough curve using a numerical fitting routine. In general, we found that the estimated filtration parameters follow the clean bed filtration model, although with a lower filtration efficiency overall. *INDEX TERMS:* 1832 Hydrology: Groundwater transport; 1829 Hydrology: Groundwater hydrology; 1831 Hydrology: Groundwater quality; *KEYWORDS:* colloid, saturated flow, size exclusion, Peclet number, dispersion, dispersivity

Citation: Keller, A. A., S. Sirivithayapakorn, and C. V. Chrysikopoulos (2004), Early breakthrough of colloids and bacteriophage MS2 in a water-saturated sand column, *Water Resour. Res.*, *40*, W08304, doi:10.1029/2003WR002676.

1. Introduction

[2] Groundwater contamination associated with the presence of suspended particles could be due either to the presence of colloids that are themselves harmful (e.g., pathogens) or to toxic substances sorbed onto the colloidal particles [*McCarthy and Zachara*, 1989; *Macler*, 1996]. Better understanding of the fate and transport of colloidal particles in the groundwater system should lead to a more accurate evaluation of health risk associated with these contaminants.

[3] The fate and transport of colloids depends on both the macroscopic and microscopic behavior of the fluid under existing flow conditions and the physicochemical conditions within the environment of the granular materials [*Ogata*, 1970]. For colloid transport in saturated porous media, researchers have found faster breakthrough of colloid particles in porous and fractured media compared with conservative tracers. These findings are observed in both column and field-scale experiments with synthetic particles, protozoa, bacteria, and viruses [e.g., *Bales et al.*, 1989; *Powelson and Gerba*, 1994; *McKay et al.*, 1999; *Harter et al.*, 2000]. Nevertheless, the early breakthrough of colloids did not happen in some cases, for instance, in the experiments by *Dong et al.* [2002] with bacteria, 1.2 × 0.6 μm in size in sand. They found that early breakthrough only occurred in sediment cores that have very fine grains with metal hydroxide coating, due probably to insufficient heterogeneity and high retention of bacteria in that particular core.

[4] *Small* [1974] demonstrated that a mixture of latex spheres of different sizes could be separated in a series of chromatographic columns packed with different solid, nonporous particles materials, such as glass beads. The results demonstrated that the larger colloids moved through the packed bed faster than the smaller ones and that the smaller packing material provided better separation between different sizes. This was called hydrodynamic chromatography (HDC), based on the finding that the rate of transport of colloidal particles through a bed packed with solid, nonporous particles depends on both colloid size and packing particle size [*Small*, 1974].

[5] The mechanism of HDC was explained by assuming finite size particles moving in a viscous fluid in the capillary [*DiMarzio and Guttman*, 1970; *Small*, 1974]. The Brownian motion of particles generates radial excursions normal to the direction of flow. Since the particles are excluded from the

0043-1397/04/2003WR002676$09.00

slowest streamlines closest to the wall, the particles move through the capillary with a mean velocity that surpasses the mean fluid velocity by a factor that increases with ratio of particle size to capillary radius. However, in a randomly packed bed, the flow channel cannot be represented simply by a series of parallel uniform tubes or slits, mainly because of sluggish diffusion that slows down the particles when they move around obstacles, such as a flow channel split around the obstacles [*Gidding*, 1978].

[6] In several colloid transport studies, early breakthrough of colloids has been described by size exclusion, in which colloids were excluded from smaller pores based on their size [e.g., *Enfield et al.*, 1989; *Abdel-Salam and Chrysikopoulos*, 1995; *Rehmann et al.*, 1999]. *Ginn* [2002] describes colloid pore inaccessibility as pore exclusion and colloid exclusion from streamlines near pore walls as size exclusion. The term differential advection was used by *Dong et al.* [2002] to explain the early breakthrough of colloids due to size exclusion, HDC, and preferential flow paths through highly conductive regions. This phenomenon was also called velocity enhancement by *Harter et al.* [2000].

[7] In this study, the term "size exclusion" refers to a combination of mechanisms related to the size of the colloid relative to the pore spaces: Size exclusion may be due to inaccessibility [*Sirivithayapakorn and Keller*, 2003] that leads to preferential pathways, or it might be due to exclusion from streamlines near the pore walls [*Auset and Keller*, 2004] that focuses the larger colloids in the central streamlines, resulting in faster velocities and straighter paths. In our pore-scale experiments we observed that under the same pressure gradient, smaller particles with a higher pore throat to colloid diameter ratio (T/C ratio) changed paths more often than larger particles. Hence smaller colloids have a more diverse path flow through a porous media [*Sirivithayapakorn and Keller*, 2003]. We also observed that for a given colloid size, higher velocity generally decreased path diversity, establishing preferential flow paths and increasing the size exclusion effect.

[8] If size exclusion plays a significant role in early breakthrough of colloids compared with a conservative tracer, as we observed at the pore scale, we would expect to see earlier breakthrough for the combination of larger size colloid and higher water velocity. In this paper we present the results from controlled column experiments that evaluated effects of differential velocities and particle sizes. These column studies were also used to upscale the results from the pore-scale observations.

2. Modeling the System

[9] One-dimensional colloid transport in homogeneous, saturated porous media with first-order adsorption (or filtration) and inactivation is governed by the following partial differential equation [*Sim and Chrysikopoulos*, 1995]:

$$\frac{\partial C(t,x)}{\partial t}+\frac{\rho}{\theta}\frac{\partial C^*(t,x)}{\partial t}=D\frac{\partial^2 C(t,x)}{\partial x^2}-U\frac{\partial C(t,x)}{\partial x}-\lambda C(t,x)-\lambda^*\frac{\rho}{\theta}C^*(t,x), \tag{1}$$

where C is the concentration of colloids in suspension; C^* is the mass of colloids adsorbed on the solid matrix; D is the hydrodynamic dispersion coefficient; U is the average interstitial velocity, assumed constant; ρ is the bulk density of the solid matrix; λ is the transformation rate constant of colloids in solution (e.g., inactivation of suspended viruses, radioactive decay of dissolved radionuclides); λ^* is the transformation rate constant of adsorbed colloids; θ is the porosity of soil medium; and t is time. The rate of colloid attachment onto the solid matrix is described by the following generalized expression:

$$\frac{\rho}{\theta}\frac{\partial C^*(t,x)}{\partial t}=r_1C(t,x)-r_2C^*(t,x), \tag{2}$$

where r_1 and r_2 are the forward and reverse rate coefficients defined as

$$r_1=k_c, \tag{3}$$

$$r_2=\frac{\rho}{\theta}(k_r+\lambda^*), \tag{4}$$

k_c is the attachment rate constant, and k_r is the detachment rate constant.

[10] The desired expression for C^* is obtained by solving equation (1) with an initial condition of zero sorbed (or filtered) colloids ($C^*(0, x) = 0$), which results in

$$C^*(t,x)=\frac{r_1\theta}{\rho}\int_0^t C(\tau,x)\exp\left[-\frac{r_2\theta}{\rho}(t-\tau)\right]d\tau. \tag{5}$$

[11] In view of equations (2) and (5), the governing equation (1) can be rewritten as

$$\frac{\partial C(t,x)}{\partial t}=D\frac{\partial^2 C(t,x)}{\partial x^2}-U\frac{\partial C(t,x)}{\partial x}-\mathrm{A}C(t,x)-\mathrm{B}\int_0^t C(\tau,x)e^{-\mathrm{H}(t-\tau)}d\tau, \tag{6}$$

where the following substitutions have been employed:

$$\mathrm{A}=r_1+\lambda, \tag{7}$$

$$\mathrm{B}=r_1(\lambda^*-\mathrm{H}), \tag{8}$$

$$\mathrm{H}=\frac{\theta r_2}{\rho}, \tag{9}$$

[12] For a semi-infinite one-dimensional porous medium in the presence of a continuous source of colloids, the appropriate initial and boundary conditions are

$$C(0,x)=0, \tag{10}$$

$$-D\frac{\partial C(t,0)}{\partial x}+UC(t,0)=\begin{cases}UC_0 & 0<t\le t_p,\\ 0 & t>t_p,\end{cases} \tag{11}$$

$$\frac{\partial C(t,\infty)}{\partial x}=0, \tag{12}$$

where C_0 is the source concentration and t_p is the duration of the solute pulse. Condition (10) establishes that there is no initial colloid concentration within the one-dimensional porous medium. The constant flux boundary (condition (11)) implies a colloid concentration discontinuity at the inlet, as we introduce a pulse of colloids. The downstream boundary condition (12) preserves concentration continuity for a semi-infinite system. Equation (6), subject to conditions (10)–(12), is solved analytically following the methods of *Chrysikopoulos et al.* [1990] and *Sim and Chrysikopoulos* [1995] to yield

$$C(t,x) = \begin{cases} \Omega(t,x) & 0 < t \le t_p, \\ \Omega(t,x) - \Omega(t-t_p,x) & t > t_p, \end{cases} \tag{13}$$

where

$$\begin{aligned} \Omega(t,x) = {} & \frac{C_0 U}{D^{1/2}} \exp\left[\frac{U_x}{2D}\right] \left\{ \int_0^t \int_0^\tau \mathrm{H} e^{-\mathrm{H}\tau} J_0\left[2(\mathrm{B}\zeta(\tau-\zeta))^{1/2}\right] \right. \\ & \cdot \left\{ \frac{1}{(\pi\zeta)^{1/2}} \exp\left[\frac{-x^2}{4D\zeta} + \left(\mathrm{H} - \mathrm{A} - \frac{U^2}{4D}\right)\zeta\right] \right. \\ & - \frac{U}{2D^{1/2}} \exp\left[\frac{Ux}{2D} + (\mathrm{H}-\mathrm{A})\zeta\right] \\ & \left. \left. \cdot \, erfc\left[\frac{x}{2(D\zeta)^{1/2}} + \frac{U}{2}\left(\frac{\zeta}{D}\right)^{1/2}\right] \right\} d\zeta s\tau \right. \\ & + e^{\mathrm{H}t} \int_0^t J_0\left[2(\mathrm{B}\zeta(t-\zeta))^{1/2}\right] \\ & \cdot \left\{ \frac{1}{(\pi\zeta)^{1/2}} \exp\left[\frac{-x^2}{4D\zeta} + \left(\mathrm{H} - \mathrm{A} - \frac{U^2}{4D}\right)\zeta\right] \right. \\ & - \frac{U}{2D^{1/2}} \exp\left[\frac{Ux}{2D} + (\mathrm{H}-\mathrm{A})\zeta\right] \\ & \left. \left. \cdot \, erfc\left[\frac{x}{2(D\zeta)^{1/2}} + \frac{U}{2}\left(\frac{\zeta}{D}\right)^{1/2}\right] \right\} d\zeta \right\}. \end{aligned} \tag{14}$$

The Bessel function relationship $I_0(z) = J_0(iz)$, where I_0 is the modified Bessel function of the first kind of zeroth order and z is an arbitrary argument [*Abramowitz and Stegun*, 1972], can be used for the evaluation of $J_0(iz)$ with complex argument. The various model parameters can be obtained by fitting experimental data to these equations using a least squares fit.

[13] The analytical solution (13) is applicable to colloid transport and is different from other published models because it separately accounts for decay/inactivation of both the suspended colloids as well as attachment/detachment to or from the solid matrix. This differentiation between the two decay/inactivation rates is important for microbial pathogens such as viruses [*Reddy et al.*, 1981; *Yates and Ouyang*, 1992; *Chrysikopoulos and Sim*, 1996; *Sim and Chrysikopoulos*, 1998; *Chrysikopoulos and Vogler*, 2004].

[14] The attachment rate constant k_c is related to the colloid filtration coefficient Φ (m^{-1}) by the following equation [*Sim and Chrysikopoulos*, 1995]:

$$k_c = U\Phi, \tag{15}$$

where Φ is the colloid filtration coefficient that can be expressed in terms of the collision efficiency α and the collector efficiency η as follows [*Yao et al.*, 1971; *Logan et al.*, 1995; *Harter et al.*, 2000]:

$$\Phi = \frac{3(1-\theta)}{2d_c}\alpha\eta, \tag{16}$$

where θ is porosity of the media and d_c is median grain size diameter (m).

[15] The collector efficiency η can be estimated using [*Rajagopalan and Tien*, 1976; *Rajagopalan et al.*, 1982; *Ryan and Elimelech*, 1996]

$$\eta = 4A_s^{1/3}N_{Pe}^{-2/3} + A_s N_{LO}^{1/8} N_R^{15/8} + 0.00338\, A_S N_G^{1.2} N_R^{-0.4}, \tag{17}$$

where A_s is a porosity dependent parameter of the Happel sphere-in-cell model [*Happel*, 1958; *Logan et al.*, 1995]

$$A_s = \frac{2(1-\gamma^5)}{2-3\gamma+3\gamma^5-2\gamma^6} \tag{18}$$

$$\gamma = (1-\theta)^{1/3} \tag{19}$$

[16] D_∞ is the colloid bulk diffusion coefficient, estimated from the Stokes-Einstein equation [*Russel et al.*, 1989]. N_{LO}, N_G, and N_R are dimensionless parameters defined as

$$N_{LO} = \frac{4A_{123}}{9\pi\mu d_p^2 \nu}, \tag{20}$$

$$N_R = \frac{d_p}{d_c}, \tag{21}$$

$$N_G = \frac{\left(\rho_p - \rho\right) g d_p^2}{18\mu\nu}, \tag{22}$$

$$N_{Pe} = \frac{\nu d_c}{D_\infty}, \tag{23}$$

where A_{123} is the Hamaker constant of the interacting media, 6.6×10^{-21} J [*Truesdail et al.*, 1998], d_p is the particle diameter (m), g is gravitational acceleration (9.81 m/s^2), μ is the fluid viscosity (kg/m·s), ν is the Darcian velocity (m/s), and ρ_p and ρ are the density of the particle and the density of the fluid (kg/m^3), respectively. Since the value of η is not

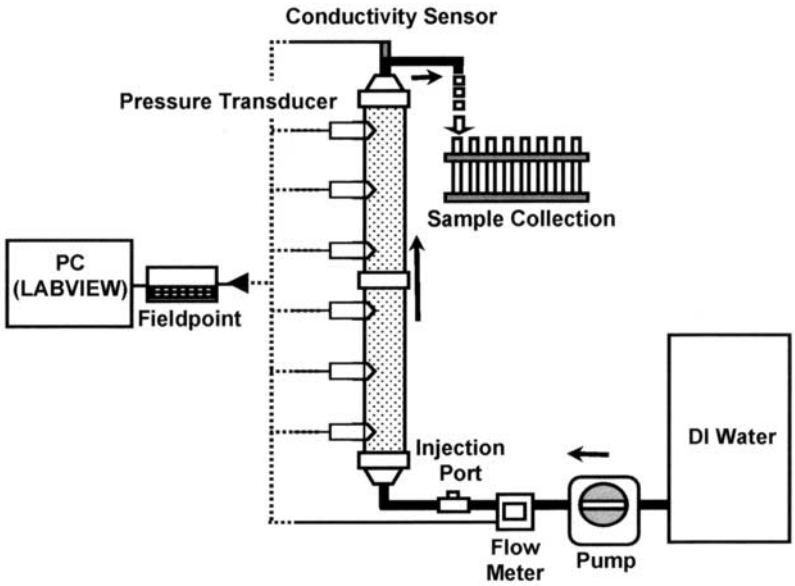

Figure 1. Experimental setup.

significantly sensitive to ρ_p, we used 1050 kg/m^3 for all colloids.

3. Materials and Methods

3.1. Experimental Methods

[17] For these experiments we used medium sand (Ward's Geology). On the basis of our characterization, the effective grain size (d_{10}) was 0.13 mm, the median grain size was 0.35 mm, and the d_{60}/d_{10} ratio was 2.92, which is not considered uniform [*Bear*, 1972]. The porosity of the sand was 0.41. The sand was first washed with mild detergent and rinsed with tap water about five times. After the detergent was rinsed, the sand was treated with 10% sulfuric acid overnight, rinsed several times with distilled water, and then oven dried overnight at 80°C. The dried sand was washed again twice with deionized water (DI). The clean sand was carefully wet pack in the column with DI water along with constant, gentle stirring to reduce stratification.

[18] The experimental setup is shown in Figure 1. The glass column was constructed with two fritted discs at top and bottom (Chemglass), used to retain the porous medium in place. Both fritted discs were 0.5 cm thick, with 40 to 60 μm average pore size. The overall column dimensions were 60 cm length and 5.0 cm inner diameter.

[19] Six pressure transducers (Sensotec, FPA/F830-02) were installed along the length of the column at equal distances of 10 cm, to measure capillary pressure during unsaturated experiments not reported here. Each transducer was calibrated before installation. A water flow meter (McMillian, 111) was installed after the peristaltic pump (SciLog, Tandem 1081). Conductivity was monitored using a conductivity sensor (Fisher Scientific model 09-326-2). Data from pressure transducers, flow meter, and conductivity sensors were collected using LabView data acquisition software (National Instruments).

[20] The experiments were conducted at flow velocities of 1.4 and 14 m/d. For the tracer experiments, we injected 50 mL of 0.01 M KCl, which was equivalent to 10% of total pore volume. Between each run the column was flushed with DI water until stable background conductivity was achieved continuously for at last 2 pore volumes. Breakthrough of the tracer was monitored continuously.

[21] For the colloid breakthrough experiments, we injected 50 mL of low ionic strength solution (~0.1 mM) with either carboxylate-modified polystyrene beads (3 and 0.05 μm) or bacteriophage MS2 virus (0.025 μm). The low ionic strength reduces attachment of colloids to the porous media [*Harter et al.*, 2000; *Kuhnen et al.*, 2000]. The initial particle concentration was in the range of 10^7–10^8 particles per milliliter. The colloid experiments were run sequentially, starting with MS2, then 0.05-μm colloids and then 3-μm colloids. The experiments were repeated five times for each colloid type at each velocity. After each run, the flow was reversed and the column was flushed at 14 m/d with DI water for at least 2 pore volumes.

[22] Colloid samples (10 mL) were collected using 12-mL borosilicate test tubes, every 2 min at the high flow rate and every 5 min at the low flow rate. The colloid particle concentrations were determined using a Spectrophotometer (Milton Roy) by measuring absorbance of the solution at 290 nm in a quartz cuvette. The actual concentrations of all samples were calculated based on direct count under epifluorescent microscopy. For MS-2, the preparation for the direct count method followed the technique described by *Hennes et al.* [1995].

3.2. Parameter Estimation

[23] There are several approaches available for parameter determination. We adopted the Levenberg-Marquardt nonlinear least squares regression method. In general, the objective of the nonlinear least squares method is to obtain estimates of the model parameters that minimize the residual sum of squares between simulated and observed data. The nonlinear least squares regression program COLLOIDFIT was developed in order to fit the colloid transport model (13) to the experimental data. COLLOIDFIT is used to deter-

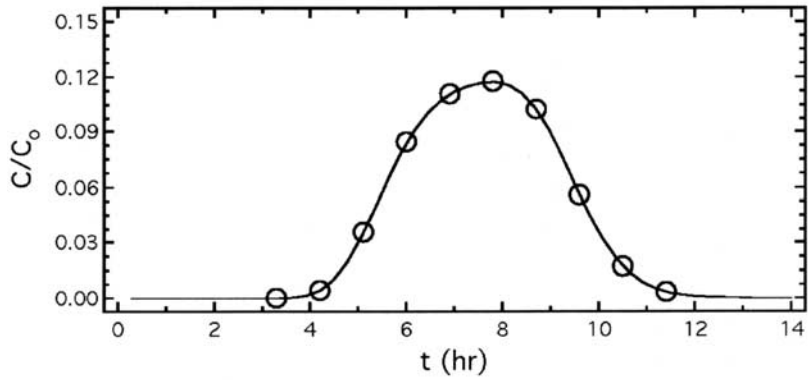

Figure 2. Artificial normalized concentration data (open circles) and breakthrough curve (solid curve) fitted by COLLOIDFIT.

mine dispersion, filtration/attachment, and transformation parameter values. COLLOIDFIT utilizes the subroutine mrqmin [*Press et al.*, 1992] for fitting the data and subroutines qdag and twodq [*IMSL*, 1991] for numerical evaluation of the single and double integrals, respectively, present in equation (14).

[24] To test the COLLOIDFIT program, artificial breakthrough data generated by the analytical solution (13) were used for the estimation of U and D. The artificial data were generated with the following parameter values: x = 150 cm, U = 25.8 cm/h, D = 48.1 cm^2/h, λ = 0.07 h^{-1}, λ^* = 0.025 h^{-1}, k_c = 0.3 h^{-1}, k_r = 0.00005 h^{-1}, θ = 0.3, ρ = 1.86 g/cm^3, and t_p = 4 hours. As shown in Figure 2, the artificial data and the fitted breakthrough curve are in excellent agreement.

[25] The fitting procedure is to provide the experimental values for ρ, θ, C_o, and t_p to COLLOIDFIT, as well as the breakthrough curve data for a given experiment. COLLOIDFIT estimates any of the six coefficients (U, D, k_c, k_r, λ, λ^*), although no more than three parameters should be fitted at a time. The parameters are estimated based on full breakthrough curve fitting, not simply the peak arrival time. Experimental data are fitted by nonlinear least squares. For these experiments, $\lambda = \lambda^* = 0$, since these colloids experience no transformation in either phase. COLLOIDFIT then iterates on the parameters to be estimated until the experimental and simulated breakthrough curves match within a certain acceptable fitting error.

[26] The η is estimated using experimental or calculated values in equations (17)–(23). Then, the fitted value of k_c from COLLOIDFIT is used to estimate Φ and α from equations (15) and (16). At this timescale, k_r was essentially negligible for all colloids.

4. Results and Discussion

[27] Average breakthrough curves from all experiments for each colloid type are presented in Figures 3 and 4, at 1.4 and 14 m/d average water velocities, respectively. For comparison, the corresponding tracer breakthrough is also presented. The breakthrough curves exhibit the combined effect of size exclusion and filtration. If only filtration were occurring, the breakthrough curve would be attenuated but would not arrive earlier than the conservative tracer [e.g., *Deborde et al.*, 1999; *Zhang et al.*, 2001]. This is very clear for all colloids at low flow velocities (Figure 3) and for larger colloids at high flow velocities (Figure 4), even within the experimental variability. For the smaller colloids (MS2 and 0.05 μm), a visual interpretation would not be sufficient to discern between filtration and size exclusion, mostly because size exclusion is less important for the smaller colloids. Larger colloids exhibit earlier breakthrough, as well as increasing filtration, as observed by *Small* [1974] and *Massei et al.* [2002]. In all cases the tracer is slower than the colloids.

[28] We present average and standard deviation for mass recovered, colloid velocity enhancement and mean arrival time in Table 1, for all experiments at the two water velocities. In general, the total mass recovered for each colloid increased significantly at higher water velocity compared with lower water velocity. This is in agreement with other studies, such as that of *Lance et al.* [1982] and *Jin et al.* [1997], which found that colloid removal by filtration in column experiments is inversely related to flow velocity. Mass recovered also decreased with increasing colloid size, although the difference in mass recovered between 0.05- and 3.0-μm colloids was not significant at the lower velocity.

[29] The velocity enhancement, defined here as colloid velocity/tracer velocity, is also a function of colloid size and water velocity. As observed at the pore scale [*Auset and Keller*, 2004; *Sirivithayapakorn and Keller*, 2003], larger colloids are excluded from certain pore spaces and travel along the central streamlines, which results in shorter paths and faster average travel velocity. This effect is more pronounced at the higher flow rates.

[30] The first moment of the arrival time for all colloids is significantly less than for KCl at either water velocity, although the difference is more pronounced at higher water velocities. There was no significant difference between mean arrival times for MS2 and 0.05-μm colloids at either velocity (Table 1), indicating that they probably travel through similar pore spaces. These two small colloids are probably not constrained by the pore-size exclusion effect, since their pore throat to colloid ratio is probably larger than the cutoff ratio observed at the pore scale [*Sirivithayapakorn and Keller*, 2003]. The 3-μm particles arrived significantly faster than MS2 or 0.05-μm colloids at either velocity. This could be due to the fact that 3-μm colloids have a lower pore throat to colloid ratio, compared with MS2 and

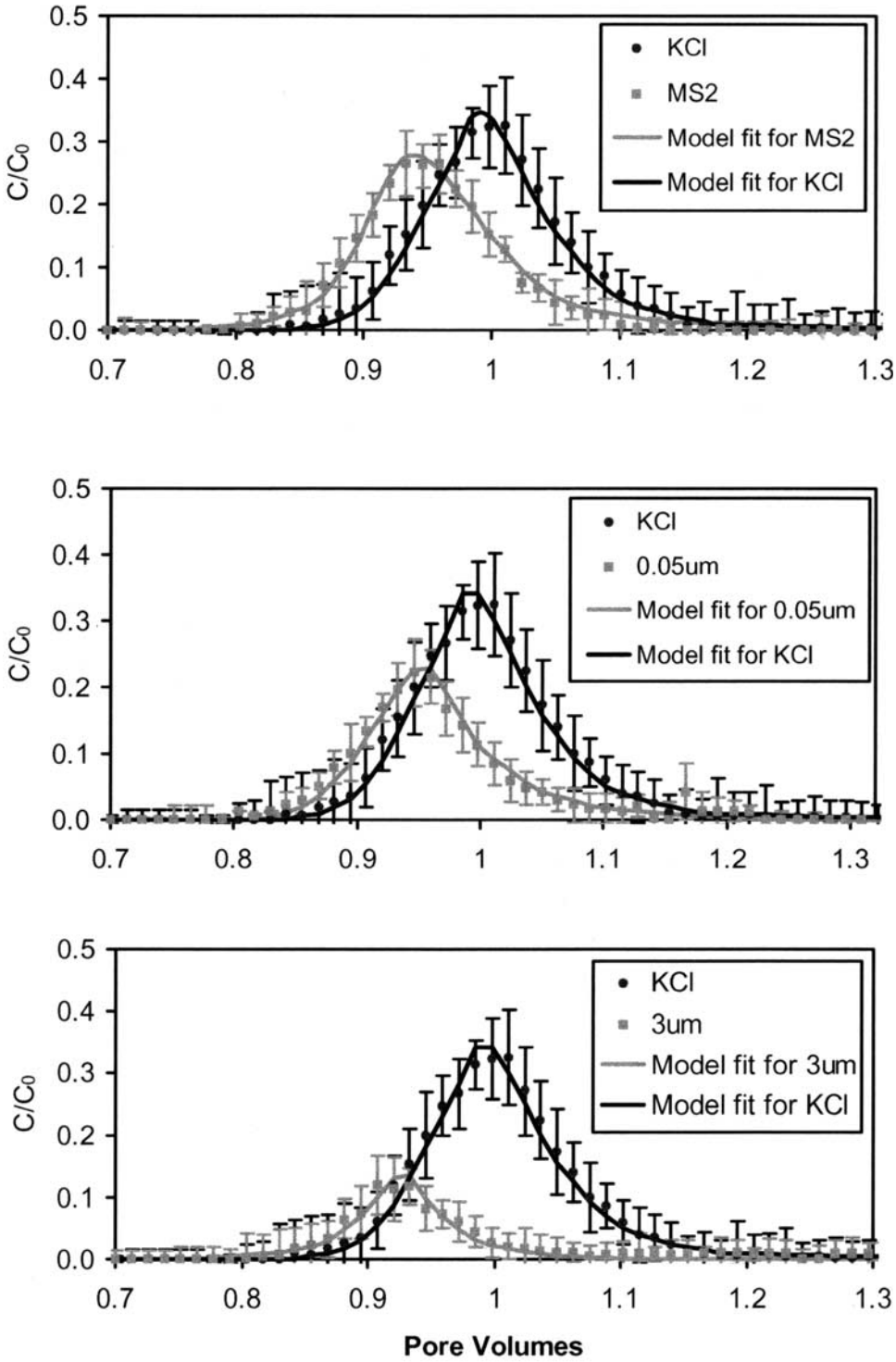

Figure 3. Average breakthrough curves from experiments conducted at 1.4 m/d average water velocity with standard deviation (five experiments each for KCl and each colloid type).

the 0.05-μm colloids, resulting in increased preferential flow paths.

[31] Average values of D for KCl are 1.96×10^{-8} at 1.4 m/d and 2.32×10^{-7} m^2/s at 14 m/d. The dispersivity δ of the medium was calculated according to *Bear* [1972] by simply dividing D by U, ignoring molecular diffusion, which we estimated to be orders of magnitude smaller. The dispersivity of the media calculated from these two flow rates is 1.3 mm (±0.1 mm).

[32] The fitted colloid dispersion coefficients from all experiments are plotted in Figure 5. Colloid dispersion depends strongly on both colloid diameter and average water velocity. Although there is variation in the dispersion coefficient from run to run, as indicated by the error bars, D

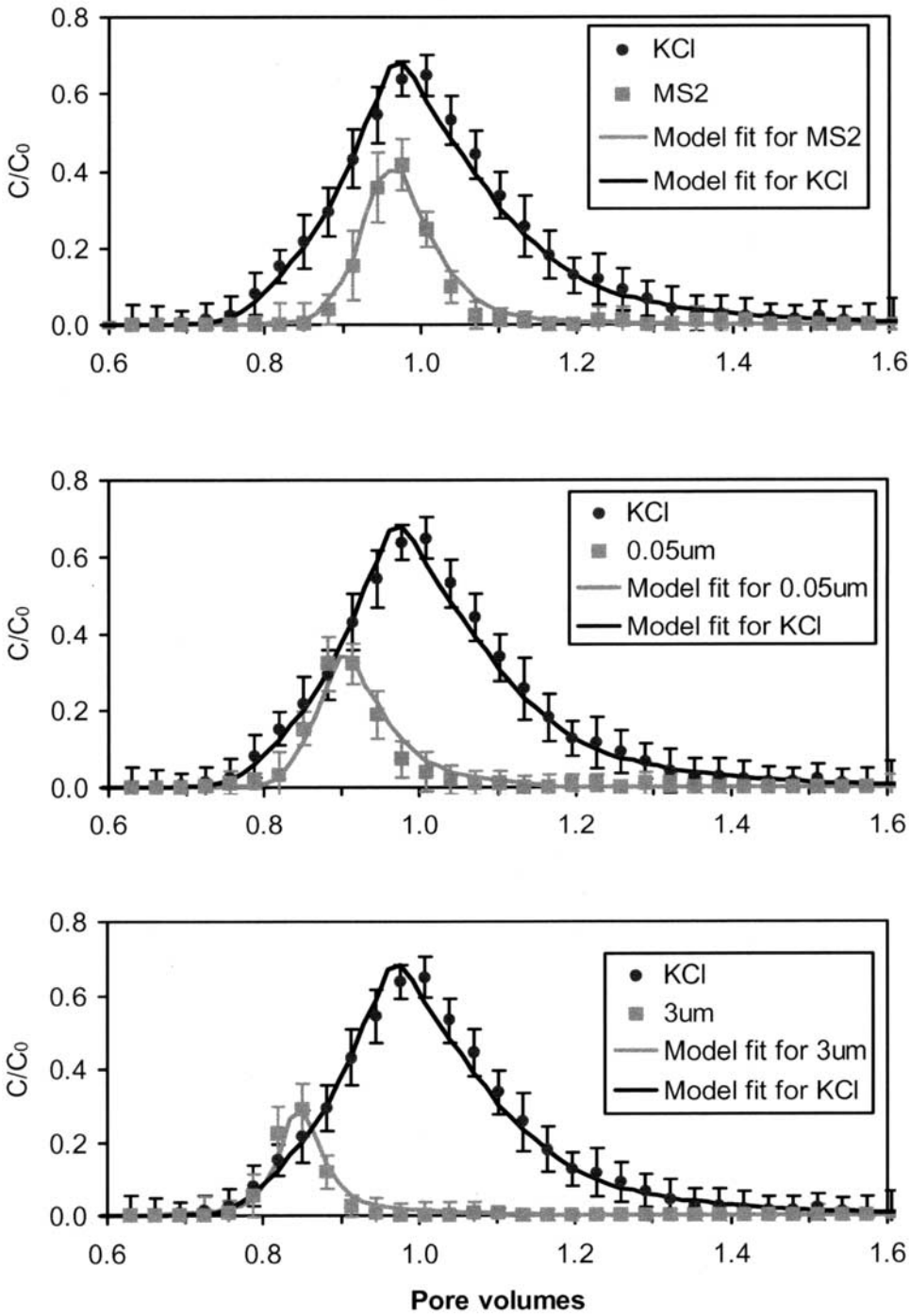

Figure 4. Average breakthrough curves from experiments conducted at 14 m/d average water velocity with standard deviation (five experiments each for KCl and each colloid type).

decreases with colloid size. The relationship between D and the size of colloids is noticeable, and different at both flow velocities, as the regressions in Figure 5 indicate. D decreases more sharply with colloid size at the higher velocities. Nevertheless, the influence of colloid size on D seems to be less as colloids become larger. Physically, this implies that there is a physical limit to the transport of large particles in the porous medium due to more restricted paths. This is in agreement with our pore-scale observations that mechanical dispersion is smaller for larger colloids since they sample less diverse flow paths [*Sirivithayapakorn and Keller*, 2003]. The smaller particles can enter a much greater number of pore spaces, thus entering more regions of high or low velocity, increasing their dispersion, while large particles are confined to those paths where the pore throat is large enough to allow their passage without filtering them out.

[33] We also calculate the dispersivity δ dividing dispersion by average water velocity. The δ is considered a property of the porous medium for solute transport in a

Table 1. Statistics of Breakthrough Behavior at Two Water Velocities (1.4 and 14 m/d)

	KCl		MS2 Virus (0.025 μm)		0.05-μm Colloids		3-μm Colloids	
	1.4 m/d	14 m/d	1.4 m/d	14 m/d	1.4 m/d	14 m/d	1.4 m/d	14 m/d
Mass recovered, %	92.3	91.7	28.8	41.0	22.2	40.2	21.3	29.1
Standard deviation	2.14	2.48	0.58	0.12	0.73	1.10	1.77	1.21
Velocity enhancement	1	1	1.05	1.11	1.05	1.11	1.09	1.14
Standard deviation	-	-	0.01	0.02	0.02	0.03	0.01	0.02
Mean arrival time (pore volumes)	1.02	1.02	0.97	0.92	0.97	0.91	0.94	0.86
Standard deviation	0.01	0.02	0.01	0.01	0.01	0.01	0.01	0.01

saturated system [*Padilla et al.*, 1999]. However, for colloids, δ is not constant and shows a dependency on colloid size (Figure 6). It might be more appropriate to consider an "effective" dispersivity when modeling colloid transport. At the lower water velocity (N_{Pe} from 14 to 80 for all colloids), δ decreases significantly as the colloids become larger. At the higher velocity (N_{Pe} from 87 to 520 for all colloids), the values of δ decrease slightly as the colloids become larger (Figure 6). This difference in behavior at different N_{Pe} might indicate that colloids sample fewer paths at the higher velocity, i.e., higher N_{Pe}. Once more, this seems to agree with the observation at the pore scale that colloids have less diverse pathways at higher velocities [*Sirivithayapakorn and Keller*, 2003].

[34] Earlier breakthrough of the colloid pulse is thus a result of faster average pore velocity and less dispersion compared with the tracer. This is in line with the observation at the field scale by *Grindrod et al.* [1996] and *Sinton et al.* [2000] and is more pronounced for the 3-μm colloids at higher velocities. These findings are also in agreement with the results derived from mathematical modeling of effective velocity and effective dispersion by *James and Chrysikopoulos* [2003].

[35] In a mathematical simulation of colloid transport in a fractured plane [*Abdel-Salam and Chrysikopoulos*, 1995], size exclusion due to variable fracture aperture was predicted to enhance the dispersion of colloids. These simulations might only capture the hydrodynamic effects of aperture variability, but not the size exclusion effect due to increased colloid size. Without size exclusion, the higher value of D for a given length and water velocity would yield faster breakthrough of the peak but the distribution of colloids would be different.

[36] In contrast, the recent attempt by *Scheibe and Wood* [2003] to model size exclusion using particle-tracking techniques indicates that the "truncation" of velocity distributions of colloids due to size exclusion may result in significant decrease in colloid (e.g., viruses and bacteria in their example) arrival times relative to a bromide tracer, and decreased dispersion, which is in line with our results. Truncation is probably related to the T/C ratio, although *Scheibe and Wood* [2003] did not explore that relationship.

[37] Table 2 presents the values of k_c derived from the experiments using COLLOIDFIT and calculated values of Φ and α, using equations (15) and (16) and experimental data for calculating η. Colloid filtration rates as measured by k_c or Φ increase with particle size and are significantly different even for MS2 and 0.05-μm colloids at the higher flow rate (Table 2). The values of k_c for MS2 from these experiments are 1.42 d^{-1} at 1.4 m/d and 1.02 d^{-1} at 14 m/d. Values of k_c for MS2 in field experiments have been reported from 0.8 to 4.1 d^{-1} at a pore water velocity of about 1.5 m/d [*Schijven et al.*, 1999].

[38] Φ decreases significantly with water velocity; *Harter et al.* [2000] observed a similar trend. From our experiments, the estimated value of Φ is in the range of 0.98–2.10 m^{-1} at 1.4 m/d and 0.07–0.14 m^{-1} at 14 m/d (Table 2).

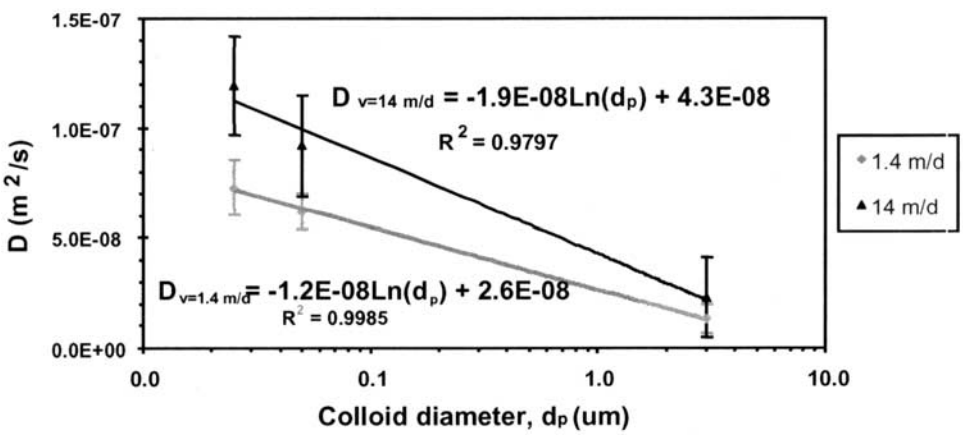

Figure 5. Average dispersion coefficients as a function of particle diameter and water velocity. Bars indicate one standard deviation.

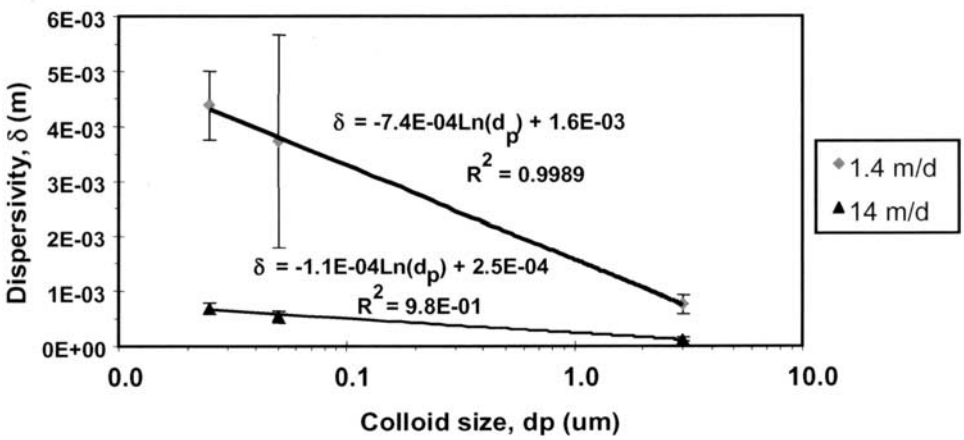

Figure 6. Average dispersivity as a function of particle diameter and water velocity. Bars indicate one standard deviation.

The values of Φ observed by *Harter et al.* [2000] for *Cryptosporidium parvum* in sandy soils and aquifer sediments are 3–61 m^{-1}, which is higher than the value observed here for 3-μm colloids at comparable flow velocities. The differences could be due to the combination of size and nature of the media and colloids.

[39] The values of α are significantly higher for larger colloids and decrease with water velocity (Table 2). Values of α for MS2 reported by *Schijven et al.* [1999] are in the range of 0.00027–0.0014 in dune sand, in line with our results. The values of α in sand for *Cryptosporidium parvum*, about 5 μm in diameter, are 0.37–1.1 for velocities comparable to this experiment [*Harter et al.*, 2000]. The values of α in sediment cores for the bacteria *Comamonas sp.*, 1.5 × 0.6 μ m in size, are 0.003–0.025 at pore velocity of 0.94–2.28 m/d [*Dong et al.*, 2002].

[40] As expected, η is significantly lower for larger colloids as well as for higher water velocity (Table 2). The calculated values of η for MS2 from our experiments are 0.152 at 1.4 m/d and 0.0033 at 14 m/d. The values of η for sand with MS2 from a field-scale study reported by *Schijven et al.* [1999] are in the range of 0.56–0.61 for pore water velocity of about 1.5 m/d; higher attachment efficiency may be due to differences in ionic strength and surface characteristics of the different media.

[41] The lower filtration parameter values observed in these experiments compared with other studies may be a result of using very clean sand, i.e., organic content less than 0.001 as measured by us experimentally. On the basis of our experimental design, the colloids were also suspended in DI water with very low ionic strength, to minimize deposition between colloids and sand, following *Schijven and Hassanizadeh* [2000]. Our objective was to scale up our pore-scale observation of the size exclusion effect at different water velocities and colloid sizes, minimizing filtration.

5. Conclusion

[42] Early breakthrough of colloids compared with a conservative tracer can be explained in part by the size exclusion effect, which leads to a combination of phenomena including pore inaccessibility of colloids as well as travel of larger colloids through the central streamlines. Results from these experiments suggested that the earlier arrival time of colloids is a result of faster average pore velocity of colloids and less dispersion compared to a tracer, due to the preferential flow paths observed at the pore scale [*Sirivithayapakorn and Keller*, 2003]. This effect is magnified with increasing particle size or water velocity. Dispersion of colloids is significantly smaller than for tracers, and decreases with increasing particle size. Dispersivity, which is normally considered constant for a medium, also decreases with increasing particle size. For colloids, the effective dispersivity is a function of colloid size due to size exclusion, particularly at low N_{Pe}.

[43] Colloid filtration coefficient, collision efficiency, and collector efficiency are estimated from the experimental results using clean bed filtration model and one-dimensional advection-dispersion transport in porous media. In general, we found that the estimated filtration parameters are lower compared with those from others studies, probably due to low ionic strength of the solution and low organic content in the medium, since minimizing filtration was part of our experimental design.

[44] Since the early breakthrough of colloids in this medium is essentially due to hydrodynamic processes and not to chemical interactions, the observed breakthrough time decreased with increasing water velocity. Although this is a real effect, in a system with stronger chemical

Table 2. Estimated Values of Filtration Parameters at Two Water Velocities (1.4 and 14 m/d)

	MS2		0.05-μm Colloid		3-μm Colloid	
	1.4 m/d	14 m/d	1.4 m/d	14 m/d	1.4 m/d	14 m/d
k_c, d^{-1}	1.42	1.02	1.43	1.11	3.12	2.17
Standard deviation	0.09	0.13	0.08	0.09	0.12	0.18
Φ, m^{-1}	0.98	0.07	1.00	0.08	2.10	0.14
Standard deviation	0.07	0.01	0.06	0.01	0.08	0.01
α	0.0026	0.0008	0.0041	0.0015	0.1026	0.0306
Standard deviation	0.0002	0.0001	0.0002	0.0001	0.0038	0.0025
η	0.152	0.0033	0.096	0.021	0.008	0.002
Standard deviation	0.0001	0.0002	0.0003	0.0001	0.0008	0.001

sorption other processes might balance the hydrodynamic effect on colloid acceleration.

[45] Our results indicate good correspondence with observations at the pore scale and suggest a mechanistic basis for understanding the movement of colloids in saturated porous media in regards to the size exclusion phenomenon.

[46] **Acknowledgment.** The authors acknowledge partial funding from U.S. EPA Exploratory Research grant R826268 and U.S. EPA grant R827133, as well as from the University of California Water Resources Center and the UCSB Academic Senate.

References

Abdel-Salam, A., and C. V. Chrysikopoulos (1995), Modeling of colloid and colloid-facilitated contaminant transport in a 2-dimensional fracture with spatially-variable aperture, *Transp. Porous Media*, *20*, 197–221.

Abramowitz, M., and I. A. Stegun (1972), *Handbook of Mathematical Functions*, 1046 pp., Dover, Mineola, N. Y.

Auset, M., and A. A. Keller (2004), Pore-scale processes that control dispersion of colloids in saturated porous media, *Water Resour. Res.*, *40*, W03503, doi:10.1029/2003WR002800.

Bales, R. C., C. P. Gerba, G. H. Grondin, and S. L. Jensen (1989), Bacteriophage transport in sandy soil and fractured tuff, *Appl. Environ. Microbiol.*, *55*, 2061–2067.

Bear, J. (1972), *Dynamics of Fuids in Porous Media*, Dover, Mineola, N. Y.

Chrysikopoulos, C. V., and Y. Sim (1996), One-dimensional virus transport in homogeneous porous media with time dependent distribution coefficient, *J. Hydrol.*, *185*, 199–219.

Chrysikopoulos, C. V., and E. T. Vogler (2004), Estimation of time dependent virus inactivation rates by geostatistical and resampling techniques: Application to virus transport in porous media, *Stochastic Environ. Res. Risk Assess.*, *18*(2), 67–78.

Chrysikopoulos, C. V., P. V. Roberts, and P. K. Kitanidis (1990), One-dimensional solute transport in porous media with partial well-to-well recirculation: Application to field experiments, *Water Resour. Res.*, *26*(6), 1189–1195.

Deborde, D. C., W. W. Woessner, Q. T. Kiley, and P. Ball (1999), Rapid transport of viruses in a floodplain aquifer, *Water Res.*, *33*(10), 2229–2238.

DiMarzio, E. A., and C. M. Guttman (1970), Separation by flow, *Macromolecules*, *3*, 131–146.

Dong, H. L., T. C. Onstott, M. E. Deflaun, M. E. Fuller, T. D. Scheibe, S. H. Streger, R. K. Rothmel, and B. J. Mailloux (2002), Relative dominance of physical versus chemical effects on the transport of adhesion-deficient bacteria in intact cores from South Oyster, Virginia, *Environ. Sci. Technol.*, *36*, 891–900.

Enfield, C. G., G. Bengtsson, and R. Lindqvist (1989), Influence of macromolecules on chemical transport, *Environ. Sci. Technol.*, *23*, 1278–1286.

Gidding, J. C. (1978), Displacement and dispersion of particles of finite size in flow channels with lateral forces: Field-flow fractionation and hydrodynamic chromatography, *Sep. Sci. Technol.*, *13*, 241–254.

Ginn, T. R. (2002), A travel time approach to exclusion on transport in porous media, *Water Resour. Res.*, *38*(4), 1041, doi:10.1029/2001WR000865.

Grindrod, P., M. S. Edwards, J. J. W. Higgo, and G. M. Williams (1996), Analysis of colloid and tracer breakthrough curves, *J. Contam. Hydrol.*, *21*, 243–253.

Happel, J. (1958), Viscous flow in multiparticle systems: Slow motion of fluids relative to bed of spherical particles, *AIChE J.*, *4*, 197–201.

Harter, T., S. Wagner, and E. R. Atwill (2000), Colloid transport and filtration of *Cryptosporidium parvum* in sandy soils and aquifer sediments, *Environ. Sci. Technol.*, *34*, 62–70.

Hennes, K. P., C. A. Suttle, and A. M. Chan (1995), Fluorescently labeled virus probes show that natural virus populations can control structure of marine microbial communities, *Appl. Environ. Microbiol.*, *61*, 3623–3627.

IMSL (1991), *IMSL MATH/LIBRARY User's Manual*, version 2.0, Visual Numerics, Houston, Tex.

James, S. C., and C. V. Chrysikopoulos (2003), Effective velocity and effective dispersion coefficient for finite-sized particles flowing in a uniform fracture, *J. Colloid Interface Sci.*, *263*, 288–295.

Jin, Y., M. V. Yates, S. S. Thompson, and W. A. Jury (1997), Sorption of viruses during flow through saturated sand columns, *Environ. Sci. Technol.*, *31*, 548–555.

Kuhnen, F., K. Barmettler, S. Bhattacharjee, M. Elimelech, and R. Kretzschmar (2000), Transport of iron oxide colloids in packed quartz sand media: Monolayer and multilayer deposition, *J. Colloid Interface Sci.*, *231*, 32–41, doi:10.1006/jcis.2000.7097.

Lance, J. C., C. P. Gerba, and D.-S. Wang (1982), Comparative movements of different enteroviruses in soil column, *J. Environ. Qual.*, *11*, 347–350.

Logan, B. E., D. G. Jewett, R. G. Arnold, E. J. Bouwer, and C. R. O'Melia (1995), Clarification of clean-bed filtration models, *J. Environ. Eng.*, *121*, 869–873.

Macler, B. A. (1996), Developing the ground water disinfection rule, *AWWA J.*, *88*, 47–55.

Massei, N., M. Lacroix, H. Q. Wang, and J.-P. Dupont (2002), Transport of particulate material and dissolved tracer in a highly permeable porous medium: Comparison of the transfer parameters, *J. Contam. Hydrol.*, *57*, 21–39.

McCarthy, J. F., and J. M. Zachara (1989), Subsurface transport of contaminants—Mobile colloids in the subsurface environment may alter the transport of contaminants, *Environ. Sci. Technol.*, *23*, 496–502.

McKay, L. D., W. E. Sanford, and J. M. Strong (1999), Field-scale migration of colloidal tracers in a fracture shale saprolite, *Ground Water*, *38*, 139–147.

Ogata, A. (1970), Theory of dispersion in a granular medium: A review of the theoretical aspects of dispersion of fluid flowing through a porous material, *U. S. Geol. Surv. Prof. Pap., 411-I*, 34 pp.

Padilla, I. Y., T.-C. J. Yeh, and M. H. Conklin (1999), The effect of water content on solute transport in unsaturated porous media, *Water Resour. Res.*, *35*, 3303–3313.

Powelson, D. K., and C. P. Gerba (1994), Virus removal from sewage effluents during saturated and unsaturated flow-through soil columns, *Water Res.*, *28*, 2175–2181.

Press, W. H., S. A. Teukolsky, W. T. Vetterling, and B. P. Flannery (1992), *Numerical Recipes in Fortran 77: The Art of Scientific Computing*, 931 pp., Cambridge Univ. Press, New York.

Rajagopalan, R., and C. Tien (1976), Trajectory analysis of deep-bed filtration with the sphere-in-cell porous media model, *AIChE J.*, *22*, 523–533.

Rajagopalan, R., C. Tien, R. Pfeffer, and G. Tardos (1982), Letter to the editor, *AIChE J.*, *28*, 871–872.

Reddy, K. R., R. Khaleel, and M. R. Overcash (1981), Behavior and transport of microbial pathogens and indicator organisms in soils treated with organic wastes, *J. Environ. Qual.*, *10*(3), 255–266.

Rehmann, L. L. C., C. Welty, and R. W. Harvey (1999), Stochastic analysis of virus transport in aquifers, *Water Resour. Res.*, *35*, 1987–2006.

Russel, W. B., D. A. Saville, and W. R. Schowalter (1989), *Colloidal Dispersion*, Cambridge Univ. Press, New York.

Ryan, J. N., and M. Elimelech (1996), Colloid mobilization and transport in groundwater, *Colloids Surf. Physicochem. Eng. Aspects*, *107*, 1–56.

Scheibe, T. D., and B. D. Wood (2003), A particle-based model of size or anion exclusion with application to microbial transport in porous media, *Water Resour. Res.*, *39*(4), 1080, doi:10.1029/2001WR001223.

Schijven, J. F., and S. M. Hassanizadeh (2000), Removal of viruses by soil passage: Overview of modeling, processes, and parameters, *Crit. Rev. Environ. Sci. Technol.*, *30*, 49–127.

Schijven, J. F., W. Hoogenboezem, and S. M. Hassanizadeh (1999), Modeling removal of bacteriophages MS2 and PRD1 by dune recharge at Castricum, Netherlands, *Water Resour. Res.*, *35*, 1101–1112.

Sim, Y., and C. V. Chrysikopoulos (1995), Analytical models for one-dimensional virus transport in saturated porous media, *Water Resour. Res.*, *31*(5), 1429–1437. (Correction, *Water Resour. Res., 32*(5), 1473, 1996.)

Sim, Y., and C. V. Chrysikopoulos (1998), Three-dimensional analytical models for virus transport in saturated porous media, *Transp. Porous Media*, *30*(1), 87–112.

Sinton, L. W., M. J. Noonan, R. K. Finlay, L. Pang, and M. E. Close (2000), Transport and attenuation of bacteria and bacteriophages in an alluvial gravel aquifer, *N. Z. J. Mar. Freshwater Res.*, *34*, 175–186.

Sirivithayapakorn, S., and A. Keller (2003), Transport of colloids in saturated porous media: A pore-scale observation of the size exclusion effect and colloid acceleration, *Water Resour. Res.*, *39*(4), 1108, doi:10.1029/2002WR001583.

Small, H. (1974), Hydrodynamic chromatography: A technique for size analysis of colloidal particles, *J. Colloid Interface Sci.*, *48*, 147–161.

Truesdail, S. E., J. Lukasik, S. R. Farrah, D. O. Shah, and R. B. Dickinson (1998), Analysis of bacterial deposition on metal (hydr)oxide-coated sand filter media, *J. Colloid Interface Sci.*, *203*(2), 369–378.

Yates, M. V., and Y. Ouyang (1992), VIRTUS, a model of virus transport in unsaturated soils, *Appl. Environ. Microbiol.*, *58*(5), 1609–1616.

Yao, K., M. T. Habibian, and C. R. O'Melia (1971), Water and wastewater filtration: Concepts and applications, *Environ. Sci. Technol.*, *5*(11), 1105–1112.

Zhang, P., W. P. Johnson, M. J. Piana, C. C. Fuller, and D. L. Naftz (2001), Potential artifacts in interpretation of differential breakthrough of colloids and dissolved tracers in the context of transport in a zero-valent iron permeable reactive barrier, *Ground Water*, *39*(6), 831–840.

C. V. Chrysikopoulos, Department of Civil and Environmental Engineering, University of California, Irvine, Irvine, CA 92697, USA.

A. A. Keller and S. Sirivithayapakorn, Bren School of Environmental Science and Management, University of California, Santa Barbara, 3420 Bren Hall, Santa Barbara, CA 93106, USA. (keller@bren.ucsb.edu)